Novel periodic dielectric ring waveguide and design of compact dual wavelength demultiplexer

Haibin Chen (陈海滨)[1*], Guohui Wang (王国珲)[1], Honglu Hou (侯宏录)[1], and Hui Wang (王 慧)[2]

[1]*School of optoelectronics Engineering, Xi'an Technological University, Xi'an 710021, China*

[2]*School of Mathematics and Statistics, Xidian University, Xi'an 710071, China*

[*]*Corresponding author: haibinn@gmail.com*

Received January 10, 2014; accepted April 23, 2014; posted online June 25, 2014

A novel one dimensional periodic dielectric ring waveguide (PDRWG) is proposed and its dispersion properties are studied in details. Based on the proposed waveguide structure, a compact dual wavelength demultiplexer is designed. By a finite-difference time-domain (FDTD) simulation method, the performance of the designed device is calculated and analyzed. The dual wavelength demultiplexer can split the communication wavelengths of 1.31 and 1.55 μm into different waveguides and output from different ports with relative high transmittances of about 98% and 92%, respectively. The PDRWG may find applications in multi-wavelength demultiplexers or other novel integrated photonic devices.

OCIS codes: 130.2790, 130.3120.

doi: 10.3788/COL201412.071301.

Dielectric waveguides are the most fundamental components for the connection of various photonic integrated devices, and many important devices in photonic integrated circuits (PICs) are generally in the form of dielectric waveguide structures. Thus, their performances directly affect the working of PICs as a whole. Light confinement of traditional dielectric waveguides in general is relatively weak, which makes the PIC size cannot be effectively reduced, for the reason that if the waveguide bending angles are too acute, great bending losses will be introduced, and many bends of the waveguide are inevitably needed in the conventional connection of PIC devices.

Periodic dielectric materials including photonic crystals have increased human control abilities on propagation behaviours of light to a new level[1,2]. For the strong confinement of light by photonic bandgaps[3], dielectric optical waveguides based on photonic crystal platforms show the advantages of compact structure, abrupt bend with negligible losses[4,5], which makes photonic crystal waveguides great advantages in the design of novel PIC devices, and especially, may greatly increase the integrating density. But optical dielectric waveguides based on photonic crystals are very complex structures, which makes the fabrication process very complex and difficult. Currently, two dimensional photonic crystal waveguides are still in the lab stage relatively far from the real applications.

At the same time, one dimensional periodic dielectric waveguides with much simpler structures than the photonic crystal waveguides have also attracted many attentions of researchers[6−22]. By a theoretical study based on numerical simulation, Luan *et al.*[7] show that a kind of one dimensional periodic dielectric rod waveguide can achieve high transmission even with acute angle bend. In a bend radius of 3λ (λ is the wavelength), a transmittivity of better than 90% is achieved, which are difficult for conventional waveguides. In 2010, Feng *et al.*[8] experimentally studied the cross connection of two perpendicular periodic dielectric waveguides based on the silicon on insulator (SOI) platform. In their experiment, the cross connection region was less than 4×4 (μm) and the two waveguide perpendicularly crossed each other, but the experimental results showed that in a wavelength range of 1520−1600 nm, the crosstalk between the two waveguides was less than −40 dB. The current researches on periodic dielectric waveguides show that the waveguide structure may be used to substitute conventional dielectric waveguides with the advantage of greatly decreasing PIC sizes without the need of complex two dimensional photonic crystal waveguides. Thus the complexities and difficulties of the fabrication process will be greatly reduced.

Besides the potential in greatly reducing PIC sizes, periodic dielectric waveguides may also be helpful for the development of new PIC devices. Many PIC devices like compact beamsplitters[9], wavelength demultiplexers[10], polarization splitters[11], optical logic devices[12], etc., based on one dimensional periodic dielectric waveguides have been proposed and studied. Although many interesting results have been achieved on the periodic dielectric waveguide, which has shown great future potentials, there are still much work to do in this area.

In this letter, a novel one dimensional periodic dielectric waveguide is designed and analyzed, in which a dielectric ring structure is used as the unit cell. As far as the author knows, the waveguide structure has not been studied before, which shows a more versatile control on the dispersion properties. For convenience, in this letter, we call the novel waveguide periodic dielectric ring waveguide (PDRWG). A compact dual wavelength demultiplexer based on the PDRWG is designed and simulated. Theoretical analyses are given for the structure design of the PDRWG and the dual wavelength demultiplexer by using a two dimensional plane wave expansion (PWE) method and finite-difference time-domain (FDTD) simulation.

As shown in Fig. 1, the waveguide is composed of a one-dimensional arranged periodic dielectric rings, which

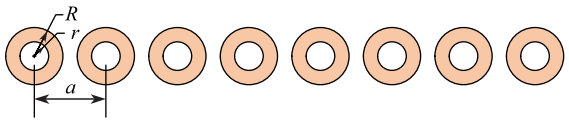

Fig. 1. (Color online) Structure of the PDRWG.

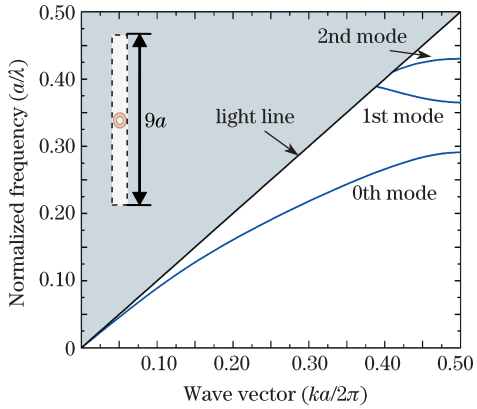

Fig. 2. (Color online) Band structure of a PDRWG with typical parameters of R=0.3a, r=0.2a.

are all with an inner radius of r and an outer radius of R. The period of the dielectric rings is a. Both the inner and outer parts of the ring structure can be light transparent dielectrics. In this letter, for simplicity, we set the inner part of the dielectric rings as air, and the outer part as GaAs. The background material is supposed as air. The refractive index of air is 1. GaAs is with a refractive index of 3.4 in the communication wavelength range without considering the dispersion.

A PDRWG can work both in the transverse electric (TE) polarization or transverse magnetic (TM) polarization. For the waveguiding propagation of light, there are no intrinsic differences between the two polarizations. Without loss of generality, only the TE polarization is considered. Based on the well known PWE method[23,24], the dispersion properties of the PDRWGs are simulated and analyzed. Band structure of a PDRWG with typical parameters of R=0.3a, r=0.2a are shown in Fig. 2. A $a \times 9a$ sized supercell shown in the inset is used for the calculation.

As seen from Fig. 2, there are three guiding modes, 0th (fundamental), 1st, and 2nd exist below the light line. They are all single mode and separated by a bandgap where no guiding mode can exist. Only waves below the light line and with a frequency in the guiding mode range can propagate in the waveguide. At the edge of the Brillouin zone of $k = 0.5 \times 2\pi/a$, all the dispersion curves become flat, which means the light with the corresponding wavelength will be stopped or trapped in the waveguide.

For a propagation constant of $k = 0.43 \times 2\pi/a$, mode distributions of the TE field $|E|^2$ are shown in Fig. 3, which show that light can be confined well in the waveguide region. Figures 3(a), (b) and (c) correspond the 0th, 1st, and 2nd mode in Fig. 2, respectively. The mode distributions of all the three guiding modes are periodic along the waveguide direction, which agree with the Bloch theorem. And in the transverse direction, all the three modes are quickly decreasing with an exponential behaviour. Although no one dielectric ring is physically connected with its neighboring components, optical waves can be effectively confined and propagated in the periodic dielectric waveguide.

The 0th mode confines the optical wave most well, and is the simplest form of mode distributions. Furthermore, in most cases, the 0th mode is enough for the fulfill of real applications. So in the following of this letter, only the 0th mode is considered for the guiding of optical waves.

There are two geometrical parameters R and r can be used to adjust dispersion properties of the PDRWG. To illustrate this, firstly, we fix R =0.4a, and adjust r from 0 to 0.35a with a step of 0.05a. The dispersion curves of the 0th modes are shown in Fig. 4(a). It shows that with the increasing of r, the curves gradually become higher and higher, and at the same time the curves bend more weakly. We also calculated another group of dispersion curves by fixing r=0.2a, and gradually increasing R from 0.25a to 0.5a with a step of 0.05a. We find an inverse tendency. That is, with the increasing of the outer radius, the curves become lower and lower, but gradually bend more and more weakly. The interesting dispersion behaviours show the versatility of the PDRWG engineering ability. Benefit from this, the PDRWGs may find some applications in novel integrated photonic devices.

Comparing the two groups of dispersion curves, it can be found that they may intersect at some frequency. As seen in Fig. 5, a PDRWG of $r_1 = 0.3a$, $R_1 = 0.39a$ (labeled as PDRWG1) intersects with a group of PDRWGs of $r_2 = 0.2a$, $R_2 = 0.29a$, 0.295a, 0.30a, and 0.305a,

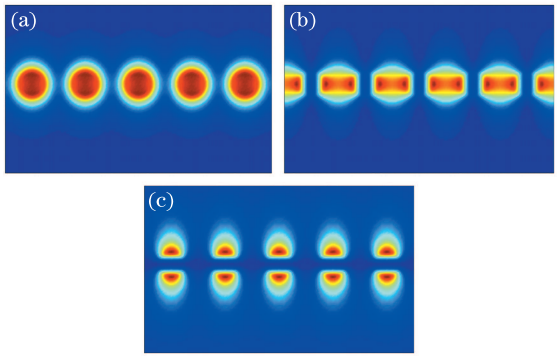

Fig. 3. (Color online) Mode distributions (the TE field $|E|^2$) of the three guiding modes at $k = 0.43 \times 2\pi/a$. Parameters of the PDRWG are the same with those of Fig. 2. (a) 0th, (b) 1st, and (c) 2nd modes.

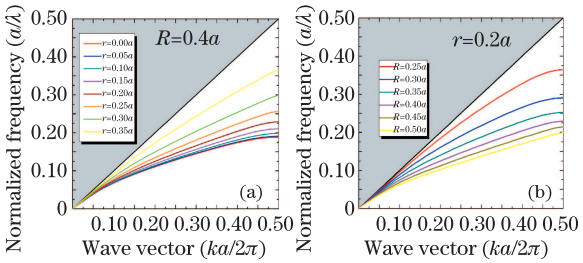

Fig. 4. (Color online) Dispersion curves for (a) parameters of R=0.4a and r=0.0a−0.35a with an increasing step of 0.05a, (b) parameters of r=0.2a and R=0.25a−0.50a with an increasing step of 0.05a.

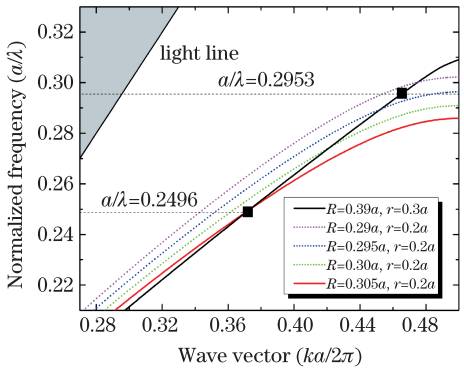

Fig. 5. (Color online) Dispersion curves intersection of the fundamental modes of two PDRWGs. One is with parameters of $R_1 = 0.39a$, $r_1 = 0.3a$. The other is with parameters of $r_2 = 0.2a$, R_2 =0.295a, 0.29a, 0.30a, and 0.305a, respectively.

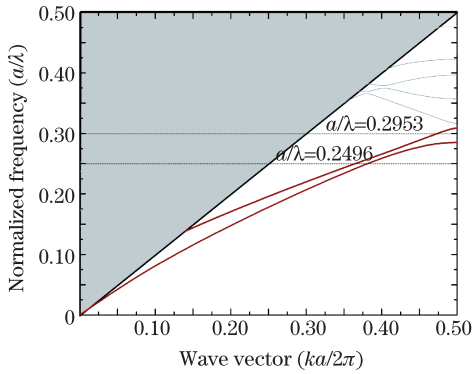

Fig. 6. (Color online) Dispersion curves of the two directional coupling PDRWGs, in which the two waveguides are arranged parallel to each other. One PDRWG is set with parameters of $R_1 = 0.39a$ and $r_1 = 0.3a$, and the other PDRWG is set with parameters of $R_2 = 0.305a$ and $r_2 = 0.2a$.

respectively. The tuning of the outer radius of the latter waveguide makes its dispersion curve cross at different frequencies with the former. For example, A PDRWG of $r_2 = 0.2a$, $R_2 = 0.305a$ (labeled as PDRWG2) is with a cross point at the normalized frequency of a/λ=0.2496 with the PDRWG of $r_1 = 0.3a$, $R_1 = 0.39a$, which means the two PDRWG with different structural parameters can be completely phase matched. According to the coupled mode theory, when the two PDRWGs are parallel arranged, light power of the corresponding frequency transported in one waveguide can be completely coupled into the other. For frequencies above or below the cross point, the two dispersion curves gradually deviate each other. It should be noted that the dispersion curve of PDRWG2 is with a cutoff frequency of a/λ=0.2860, and that of PDRWG1 is with a cutoff frequency of a/λ=0.3091. When the frequency is between the two cutoff frequencies, only one mode is supported. The power can mainly confined in the PDRWG1, and will not couple into PDRWG2. This makes us to believe that PDRWGs can be used for the design of dual wavelength demultiplexers.

Now, we consider the directional coupling of PDRWG1 and PDRWG2. Actually, for their mutual coupling, the dispersion curves will be changed more or less. We arrange the two waveguide PDRWG1 and PDRWG2 parallel to each other with a separation distance of 2a. Through the supercell based PWE method, dispersion curves of the coupling structure are calculated, as shown in Fig. 6. We can see that there are two neighboring modes, which is the result of the coupling of the fundamental 0th order modes of PDRWG1 and PDRWG2. At the frequency a/λ=0.2496, two modes exist, and at the frequency a/λ=0.2953, only one mode survives. For the frequency a/λ=0.2496, the two modes are with propagation constants of $k_0 = 0.3846 \times 2\pi/a$ and $k_1 = 0.3646 \times 2\pi/a$, respectively. According to the coupling mode theory, the corresponding light energy will coupling back and forth between PDRWG1 and PDRWG2 with a coupling length of $\pi/|k_0 - k_1| = 25a$. For the frequency a/λ=0.2953, the light energy will not coupling to PDRWG2 at all, since only one mode exists. Thus light propagating properties at the two frequencies of a/λ =0.2496 and 0.2953 described previously should be valid.

Based on the FDTD method, optical propagating behaviours of the parallel structure at the frequencies of a/λ=0.2496 and 0.2953 are simulated, as shown in Figs. 7(a) and (b), respectively. In the simulation, optical waves are excited at the center of PDRWG1 at X=0, and perfectly matched layers (PMLs) are used. The coupling length is 60a. At the frequency a/λ=0.2496, as expected, light field transported in PDRWG1 gradually reduces and in PDRWG2 gradually increases. After a propagating length of about 25a, which is approximately equal to the predication of coupling mode theory, the field in PDRWG1 almost completely disappears and reaches its greatest value in PDRWG2. By further propagating, light gradually completely couples back to PDRWG1 again. Light couples back and forth between the two PDRWGs. At the frequency a/λ=0.2953, it shows that, the light field is mainly confined in PDRWG1 and almost does not couple to PDRWG2. The weak field in PDRWG2 is actually the evanescent tail of the light field transmitted in PDRWG1. The reason for this is at the frequency a/λ=0.2953 only the PDRWG1 can support a mode to propagate, and the mode for PDRWG2 is cutoff. The results here can be directly used for the design of a dual wavelength demultiplexer.

The designed structure is shown in Fig. 8, in which

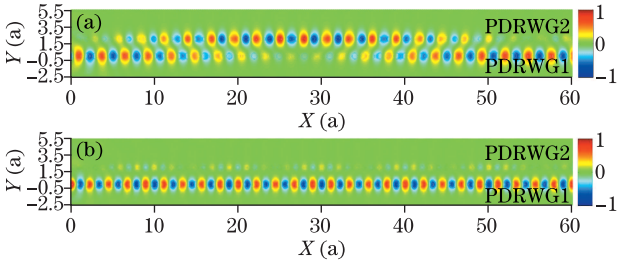

Fig. 7. (Color online) FDTD simulated steady-state field amplitude distributions at normalized frequencies of (a) a/λ=0.2496 and (b) a/λ=0.2953.

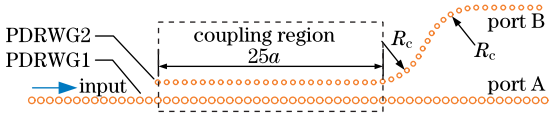

Fig. 8. (Color online) Structure of the designed dual wavelength demultiplexer.

the two coupling PDRWGs are denoted by PDRWG1 and PDRWG2 respectively. The two waveguides PDRWG1 and PDRWG2 are with the same structural parameters as previously mentioned. The separation distance of the two PDRWGs is chosen as the same value of $2.0a$. The coupling length is chosen as $25a$. At the end of the coupling region, the waveguide PDRWG1 extends along its original direction, but the PDRWG2 extends with two successive bending waveguides with a curvature radius of $R_c = 0.5a/\sin 5^\circ = 5.74a$. The two bending parts are both with a bend angle of 60°. Between them is a $3a$ length straight PDRWG. The structure arrangement makes the two waveguide separate with a distance of $10.34a$ finally, as a result they don't couple to each other any more.

If an optical signal is input in PDRWG1 from left-hand side of the structure, following previous analysis, at the wavelength $a/0.2953$, for the two waveguides will not couple at all, all the power will output from port A. At the wavelength of $a/0.2496$, the power can completely transfer from PDRWG1 into PDRWG2 and transmitted out from port B. Thus the structure can achieve the function of a dual wavelength demultiplexer. Set a=387 nm, then $R_1 = 151$ nm, $r_1 = 116$ nm, $R_2 = 118$ nm, $r_2 = 77$ nm, the structure is thus can work for the demultiplexing of the communication wavelengths of 1.55 and 1.31 μm.

To illustrate the dual wavelength demultiplexing performance, the structure is numerically simulated with a FDTD method in a steady state. The steady-state field distributions of the transverse electric field at the two designed wavelengths of 1.31 and 1.55 μm are shown in Figs. 9(a) and (b). As expected, light of the wavelength 1.31 μm can not couple into PDRWG2, but directly outputs from port A. At the wavelength 1.55 μm, after a length of $25a$ 9.7 μm, nearly all the power is coupled into PDRWG2, and outputs from port B.

To further characterize the dual wavelength demultiplexer, power transmission spectra at both port A and port B are calculated. As seen in Fig. 10, at the shorter wavelength part below 1.35 μm, more than 96.8% of the optical power is transmitted in PDRWG1 and output from port A, and only very few of the power (below

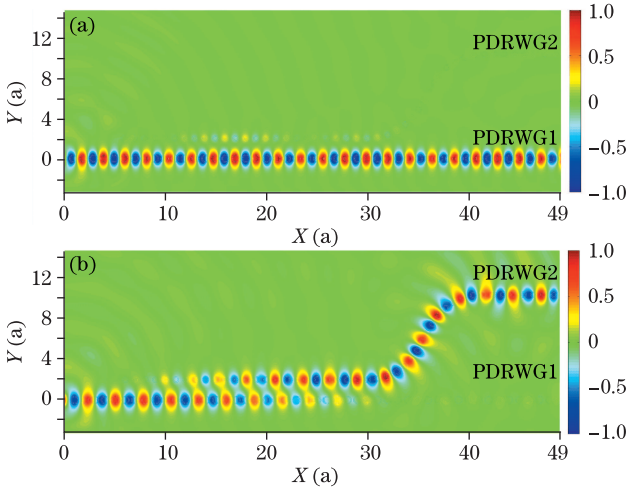

Fig. 9. (Color online) FDTD simulated steady-state field amplitude distributions at (a) 1.31 and (b) 1.55 μm.

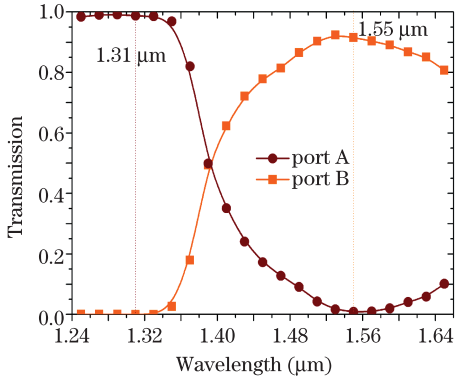

Fig. 10. (Color online) Transimission spectra of the dual wavelength demultiplexer at the two output ports A and B.

2.6%) is coupled into PDRWG2 and output from port B. Above 1.35 μm, with the increase of the wavelength, the power output from port A quickly falls down, at the same time, the power output from port B grows up evidently. When the wavelength is above 1.393 μm, the power output from B overtakes that from port A. Further increasing the wavelength, the power output from port A gradually achieves its minimum of 0.8% at 1. 55 μm and then gradually increases, and the power output from port B gradually reach its maximum of 92.4% at 1.53 μm and then gradually decreases. The transmittances at the designed wavelengths of 1.31 and 1.55 μm are 98.7% and 91.5%, respectively.

It should be noticed that the sum of the transmittances of the two ports is not 100%, especially near the wavelength 1.55 μm, nearly 8% of the power is lost. The main reason is the relatively short curvature radius R_c of PDRWG2, which results part of the optical power radiated into the free space. A calculation on the bend loss confirms a loss of 7.4% caused by the waveguide bending. And of course, the reflection or mismatching between the input waveguide and coupling region may also cause some power loss. The bending loss can be effectively reduced by carefully tuning the geometrical parameters of this part, or by the simplest way, increasing the curvature radius R_c[7]. For example, by doubling the curvature radius R_c, calculation results show that the bending loss is reduced to a low value of 1.3%.

By reducing the separation distance of the two PDRWGs, the compactness of the structure can be further increased. Our simulation shows that, with a separation distance of $1.8a$, for the wavelength 1.31 μm, the transmittance at port A is 97.4% and 0.02% is cross coupled to port B. For the wavelength 1.55 μm, the transmittances at ports B and A are 90.1% and 2.4%, respectively. The performance is close to that with $2.0a$ separation distance, but the coupling length of the demultiplexer have been reduced to $20a$ (7.7 μm).

In conclusion, a novel PDRWG is proposed and studied. The waveguide shows a more versatile control ability on the dispersion and propagation properties. Based on the waveguide, we also design a dual wavelength demultiplexer for optical communication wavelengths. The demultiplexer can effectively split the wavelength 1.31 and 1.55 μm into two different waveguides and output from different ports with transmittances of more than 98% and 92%, respectively. By further exploring the

waveguide's dispersion properties, the structure may be extended to achieve a muli-wavelength demultiplexer or other kind of novel PIC devices. The usability of the PDRWG structure can be further expanded, if some active effects are included. For example, with liquid crystals filled in the inner parts of the rings, the waveguides may be used as dynamic devices.

In this letter, for simplicity, the simulation is based on a two dimensional model. To achieve a realizable structure, the dielectric rings should be with a finite height and be fabricated on a supporting dielectric substrate with a lower refractive index. The simulation should be based on a three-dimensiona model, which will be further studied in our future research.

This work was supported by the National Natural Science Foundation of China (Nos. 61102144 and 61308071) and the Key Project of Chinese Ministry of Education (No. 212176).

References

1. S. John, Phys. Rev. Lett. **58,** 2486 (1987).
2. E. Yablonovitch, Phys. Rev. Lett. **58,** 2059 (1987).
3. S. Noda, K. Tomoda, N. Yamamoto, and A. Chutinan, Science **289,** 604 (2000).
4. H. Benisty, J. Appl. Phys. **79,** 7483 (1996).
5. A. Mekis, J. Chen, I. Kurland, S. Fan, P. Villeneuve, and J. Joannopoulos, Phys. Rev. Lett. **77,** 3787 (1996).
6. S. H. Fan, J. D Joannopoulos, J. N. Winn, A. Devenyi, J. C. Chen, and R. D. Meade, J. Opt. Soc. Am. B **12,** 1267 (1995).
7. P. G. Luan and K. D. Chang, Opt. Express **14,** 3263 (2006).
8. J. B. Feng, Q. Q. Li, and S. S. Fan, Opt. Lett. **35,** 3904 (2010).
9. P. G. Luan and K. D. Chang, Opt. Express **15,** 4536 (2007).
10. W. W. Huang, Y. Zhang, and B. J. Li, Opt. Express **16,** 1600 (2008).
11. Y. Zhang, H. X. Lei, and B. J. Li, Opt. Commun. **283,** 2140 (2010).
12. S. Q. Zeng, Y. Zhang, B. J. Li, and E. Y. Pun, Photon. Nanostruct. Fundam. Appl. **8,** 32 (2010).
13. K. K. Lee, Y. Avniel, and S. Johnson, Opt. Express **16,** 9261 (2008).
14. J. Garcia, P. Sanchis, A. Martinez, and J. Marti, Opt. Express **16,** 3146 (2008).
15. H. Yi, Y. Zhu, and Z. Zhou, Chin. Opt. Lett. **7,** 312 (2009).
16. I. Y. Polishchuk, M. I. Gozman, G. S. Blaustein, and A. L. Burin, Phys. Rev. E **81,** 026601 (2010).
17. H. T. Guo, Y. Zhang, and B. J. Li, Opt. Commun. **284,** 2292 (2011).
18. W. F. Zhang, J. H. Liu, W. P. Huang, and W. Zhao, IEEE Photon. J. **3,** 512 (2011).
19. L. Huang, B. Chen, Y. D. Li, and C. L. Liu, Appl. Opt. **51,** 3950 (2012).
20. F. Barra, V. Pagneux, and J. Zuñiga, Phys. Rev. E **85,** 016209 (2012).
21. T. Sun, Y. Jin, J. Shao, and Z. Fan, Chin. Opt. Lett. **8,** 557 (2010).
22. B. Chen, L. Huang, Y. Li, C. Liu, and G. Liu, Chin. Opt. Lett. **10,** 111301 (2012).
23. S. Johnson and J. Joannopoulos, Opt. Express **8,** 173 (2001).
24. S. Guo and S. Albin, Opt. Express **11,** 167 (2003).